Journal of Statistical Models and Methods (2026)
2(1), 49–72, https://doi.org/10.65905/w3gx5360

Article Type: Research article

Estimation of Reliability Measures for the Hjorth Model Based on Constant-Stress Accelerated Life Tests with Type-II Censoring

Abdulaziz H. Almalki[1], Mazen Nassar[1,2], Ali Algarni[1]

[1]Department of Statistics, Faculty of Science, King Abdulaziz University, Jeddah 21589, Saudi Arabia
[2]Department of Statistics, Faculty of Commerce, Zagazig University, Zagazig 44519, Egypt

Corresponding Author
Abdulaziz H. Almalki
aalmalki1601@stu.kau.edu.sa

Article History

Received: 01 April 2026
Revised: 13 May 2026
Accepted: 18 May 2026

Keywords
Reliability estimation;
Hjorth distribution;
Constant-stress accelerated life testing;
Maximum product of spacings;
Hazard rate function;
Type-II censoring

Abstract

Accelerated life testing is widely used to assess product reliability under time and cost constraints, particularly when lifetime data are subject to censoring. This paper investigates statistical inference for the Hjorth distribution under constant-stress accelerated life tests with Type-II censoring. The model parameters are estimated using maximum likelihood and maximum product of spacings methods, and asymptotic confidence intervals are constructed. The scale parameter is linked to the stress level through a log-linear relationship, enabling reliability assessment under normal operating conditions. A comprehensive Monte Carlo simulation study is conducted to evaluate the performance of the proposed estimators, and the methodology is illustrated using a real engineering dataset. The results indicate that maximum likelihood estimators provide higher efficiency for parameter estimation, whereas the maximum product of spacings method offers improved performance for reliability measures under normal use conditions. These findings highlight the complementary roles of the two estimation approaches in accelerated life testing analysis.

1 Introduction

High-reliability products used in aerospace, automotive systems, electronics, and semiconductor manufacturing are typically designed to fail rarely under nominal operating conditions. While this is desirable from an engineering standpoint, it complicates reliability assessment because few failures are observed within practical test durations. Consequently, lifetime datasets collected at use conditions are often dominated by censoring, which increases inferential uncertainty and makes traditional life testing expensive or even infeasible unless extremely long observation times or very large sample sizes are available. Accelerated life tests (ALTs) provide a practical route to obtain informative failure data within realistic time and cost constraints. The general idea is to operate test units at elevated stress levels such as increased temperature, voltage, mechanical load, or pressure so that failures occur sooner. The essential assumption is that higher stress accelerates the same underlying degradation or failure mechanisms that govern field performance, enabling the analyst to use appropriate acceleration models to extrapolate results back to normal-use conditions. This framework allows manufacturers to evaluate reliability more efficiently, identify potential design weaknesses early, and predict lifetime characteristics. Further background and statistical treatment of ALTs are provided by Meeker et al. [1] and Nelson [2].

Two ALT designs are used most frequently in practice: constant-stress ALTs (CSALTs) and step-stress ALTs (SSALTs). In a CSALT, each test unit is assigned a single fixed stress level that remains unchanged

Copyright © 2026 by the author. Published under Creative Commons Attribution (CC BY) license.

throughout the experiment; the test continues until all units fail or until a predetermined stopping rule is met. This design is attractive because it is straightforward to implement and typically leads to comparatively tractable likelihood-based inference, which explains its wide adoption in industrial settings. A significant body of literature has focused on developing and refining inferential procedures for CSALT data. For example, Abd El-Raheem [3] developed optimal design and estimation procedures for constant-stress tests under Type-I censoring assuming an extension of the exponential lifetime distribution. Kumar et al. [4] compared nine classical estimators for parameters and reliability measures in constant-stress settings and used simulation evidence to highlight efficiency differences. Further related developments appear in Wu et al. [5], Kamal et al. [6], Elwahab et al. [7], Lou et al. [8], Babu [9], Balakrishnan et al. [10], and Liu et al. [11]. In SSALTs, by contrast, the stress applied to each unit increases over time, either according to a prespecified schedule or adaptively based on the occurrence of a given number of failures. Thus, units experience progressively higher stress levels in discrete stages determined by time and/or observed failures. Although such designs can provide richer information about deterioration dynamics, they typically require more elaborate modeling and inference than CSALTs. Recent methodological work for SSALT data includes, among others, Balakrishnan et al. [12], LA et al. [13], Ling et al. [14], Rather and Ahmad [15], and Das et al. [16].

Beyond test design, a crucial aspect of reliability analysis is the selection of an appropriate lifetime distribution that adequately reflects the underlying failure behavior. In practice, reliability data often exhibit diverse hazard-rate patterns, which has motivated the development of numerous flexible lifetime models. Recent contributions in this direction include the models proposed by Shiha et al. [17], Atchadé et al. [18], Sayibu et al. [19], and Gaire and Gurung [20]. Among established models, the Hjorth (Hj) distribution introduced by Hjorth [21] has received considerable attention due to its ability to accommodate several important shapes of the hazard rate function (HRF), including decreasing, increasing, and bathtub forms, which frequently arise in engineering reliability applications. Although classical lifetime distributions, such as the exponential, Rayleigh, and Weibull distributions, have been widely used in reliability studies, they may impose restrictive assumptions on the HRF. For example, the exponential distribution assumes a constant hazard rate, the Rayleigh distribution is mainly suitable for increasing hazard-rate behavior, and the Weibull distribution is commonly used for relatively simple hazard-rate patterns, such as increasing or decreasing failure rates. Therefore, these models may be inadequate when the data exhibit more complex failure behavior, especially bathtub-shaped hazard rates. Guess et al. [22] studied the mean residual life properties of the Hj distribution. Subsequent work has developed inferential procedures for the two-parameter Hj model under various censoring schemes; see, for example, Yadav et al. [23], Pandey and Ali [24], Elshahhat and Nassar [25], and Alotaibi et al. [26].

Motivated by the need for flexible and robust modeling of lifetime data in accelerated life testing, this paper considers the Hj distribution due to its ability to accommodate diverse failure behaviors and a wide range of HRF shapes commonly observed in engineering applications. In the context of CSALTs, the Hj model provides a convenient and interpretable framework that remains stable across different stress levels. The objective of this study is to develop statistical inference for the Hj distribution under Type-II censoring by estimating the model parameters together with the reliability function (RF) and the HRF. Two classical estimation approaches, maximum likelihood and maximum product of spacings (MPS), are employed, and the scale parameter is linked to the stress level through a log-linear relationship to enable extrapolation to normal operating conditions. The proposed methods are evaluated through an extensive Monte Carlo simulation study and illustrated using a real engineering dataset. The main contribution lies in integrating the Hj distribution within a CSALT framework under Type-II censoring and providing a comparative analysis of point and interval inference for both model parameters and reliability measures.

The remainder of the paper is organized as follows. Section 2 introduces the Hj distribution and specifies the assumptions for CSALTs under Type-II censoring. Section 3 derives the maximum likelihood estimates (MLEs) and approximate confidence intervals (ACIs) for the parameters and reliability measures. Section 4 develops the MPS estimates (MPSEs) and their associated ACIs. Section 5 presents a simulation study comparing the two estimation methods. Section 6 applies the proposed model to a real engineering dataset. Finally, Section 7 concludes with a summary of the main findings.

2 Model and Basic Assumptions

Let X be a random variable following the Hj distribution with scale parameter λ_j and shape parameter θ. The corresponding probability density function (PDF) is given by

$$f_j(x;\boldsymbol{\zeta}) = \frac{\theta + \lambda_j x(1+x)}{(1+x)^{1+\theta}} e^{-\frac{\lambda_j}{2}x^2}, \qquad x > 0,\ \lambda_j > 0,\ \theta > 0. \tag{1}$$

where $\boldsymbol{\zeta} = (\lambda_j, \theta)^\top$, and the corresponding cumulative distribution function (CDF) is

$$F_j(x;\boldsymbol{\zeta}) = 1 - \frac{e^{-\frac{\lambda_j}{2}x^2}}{(1+x)^{\theta}}. \tag{2}$$

The RF is given by

$$R(x;\boldsymbol{\zeta}) = \frac{e^{-\frac{\lambda_j}{2}x^2}}{(1+x)^{\theta}}, \tag{3}$$

and the HRF is given by

$$H(x;\boldsymbol{\zeta}) = \lambda_j x + \frac{\theta}{1+x}. \tag{4}$$

The following assumptions are adopted for statistical inference under CSALTs with Type-II censoring using the Hj distribution:

1. A total of N identical test items are allocated to k groups with sizes $n_1, n_2, \ldots, n_k$, such that
$$N = \sum_{j=1}^{k} n_j.$$
2. The experiment is conducted at k accelerated stress levels S_j, $j = 1, 2, \ldots, k$. The stress level under normal operating conditions is denoted by S_u, and the stress levels satisfy
$$S_u < S_1 < S_2 < \cdots < S_k.$$
At stress level S_j, the jth group of n_j items is tested under a constant stress S_j.
3. Under the Type-II censoring scheme, the experiment at the jth stress level continues until a predetermined number r_j $(r_j < n_j)$ of failures are observed. Let
$$x_{1j} < x_{2j} < \cdots < x_{r_j j},\ j = 1, 2, \ldots, k,$$
denote the ordered failure times observed from the jth group. The remaining $n_j - r_j$ items are right censored at time $x_{r_j j}$.
4. The lifetimes of the test items at stress level S_j are assumed to be independent and identically distributed random variables following the Hj distribution with PDF given in (1).
5. The shape parameter θ is assumed to be invariant with respect to the stress level and is common to all accelerated conditions.
6. The scale parameter λ_j depends on the stress level through the log-linear stress–life relationship
$$\ln(\lambda_j) = a + bS_j, \qquad j = 1, 2, \ldots, k,$$
where a and b are unknown constants determined by the characteristics of the product.

Assumption 6 relates the stress level to the scale parameter through a log-linear stress–life relationship, which is widely used in accelerated life testing. This formulation reflects the common premise that higher stress primarily accelerates the failure process by compressing the time scale while preserving the underlying failure mechanism. Consequently, the stress effect is incorporated through the scale parameter λ_j, whereas the distributional shape remains governed by the common parameter θ, as specified in Assumption 5. The log-linear model is attractive because of its simplicity and interpretability, and it often

serves as a convenient approximation to physics-based acceleration models. Under appropriate stress transformations, it can be viewed as a linearized representation of the Arrhenius model for temperature-driven acceleration or the inverse power-law model for nonthermal stress factors such as voltage, load, or pressure. For these reasons, the log-linear stress–life model has been widely used in reliability practice and in methodological research on accelerated life testing.

3 Maximum Likelihood Estimation

In this section, the unknown parameters a, b, and θ are estimated using the maximum likelihood estimation method based on Type-II censored samples obtained from CSALTs. In addition, the MLEs of the RF and HRF under normal operating conditions are derived. Furthermore, the ACIs for the unknown parameters and reliability measures are constructed using the asymptotic properties of the MLEs.

3.1 Point estimation

Let x_{ij}, for $j = 1, 2, \ldots, k$ and $i = 1, 2, \ldots, r_j$, denote the observed failure times from a Type-II censored sample at stress level S_j. Using (1) and (2), the likelihood function for the parameters a, b, and θ can be written, excluding the constant term, as follows:

$$L(\boldsymbol{\Psi}) = \prod_{j=1}^{k}\prod_{i=1}^{r_j} \frac{\theta + e^{a+bS_j}x_{ij}(1+x_{ij})}{(1+x_{ij})^{1+\theta}} e^{-\frac{e^{a+bS_j}}{2}x_{ij}^2} \left[\frac{e^{-\frac{e^{a+bS_j}}{2}x_{r_jj}^2}}{(1+x_{r_jj})^{\theta}}\right]^{n_j-r_j}, \tag{5}$$

where $\boldsymbol{\Psi} = (a, b, \theta)^\top$. From (5), the log-likelihood function can be written as

$$\begin{aligned}\ell(\Psi) = &\sum_{j=1}^{k}\sum_{i=1}^{r_j}\left\{\log\left[\theta + e^{a+bS_j}x_{ij}\left(1+x_{ij}\right)\right] - (1+\theta)\log\left(1+x_{ij}\right) - \frac{e^{a+bS_j}}{2}x_{ij}^2\right\}\\ &- \sum_{j=1}^{k}(n_j - r_j)\left[\frac{e^{a+bS_j}}{2}x_{r_jj}^2 + \theta\log\left(1+x_{r_jj}\right)\right].\end{aligned} \tag{6}$$

Based on the objective function in (6), the MLEs of the unknown parameters a, b, and θ are obtained by simultaneously solving the following system of normal equations:

$$\frac{\partial\ell(\boldsymbol{\Psi})}{\partial a} = \sum_{j=1}^{k}\left\{\sum_{i=1}^{r_j}\left[\frac{e^{a+bS_j}x_{ij}\left(1+x_{ij}\right)}{\theta + e^{a+bS_j}x_{ij}\left(1+x_{ij}\right)} - A_{ij}\right] - (n_j - r_j)A_{r_jj}\right\} = 0, \tag{7}$$

$$\frac{\partial\ell(\boldsymbol{\Psi})}{\partial b} = \sum_{j=1}^{k} S_j\left\{\sum_{i=1}^{r_j}\left[\frac{e^{a+bS_j}x_{ij}\left(1+x_{ij}\right)}{\theta + e^{a+bS_j}x_{ij}\left(1+x_{ij}\right)} - A_{ij}\right] - (n_j - r_j)A_{r_jj}\right\} = 0 \tag{8}$$

and

$$\frac{\partial\ell(\boldsymbol{\Psi})}{\partial\theta} = \sum_{j=1}^{k}\left\{\sum_{i=1}^{r_j}\left[\frac{1}{\theta + e^{a+bS_j}x_{ij}\left(1+x_{ij}\right)} - \log\left(1+x_{ij}\right)\right] - (n_j - r_j)\log\left(1+x_{r_jj}\right)\right\} = 0, \tag{9}$$

where $A_{ij} = \frac{1}{2}e^{a+bS_j}x_{ij}^2$. Since the system of likelihood equations (7)–(9) does not yield explicit solutions, the Newton–Raphson method, as implemented in the R software, is adopted to compute the MLEs of a, b, and θ, namely $\hat{a}$, $\hat{b}$, and $\hat{\theta}$. Then, by the invariance property of MLEs, the estimator of the scale parameter corresponding to stress level S_j is obtained as

$$\hat{\lambda}_j = e^{\hat{a}+\hat{b}S_j}.$$

Furthermore, under the normal operating stress level S_u, the MLEs of the RF and HRF, at mission time t, are given by

$$\hat{R}_u(t) = \frac{e^{-\frac{\hat{\lambda}_u}{2}t^2}}{(1+t)^{\hat{\theta}}}$$

and

$$\hat{H}_u(t) = \hat{\lambda}_u t + \frac{\hat{\theta}}{1+t},$$

where $\hat{\lambda}_u = e^{\hat{a}+\hat{b}S_u}$ denotes the MLE of the scale parameter under normal use conditions.

3.2 Interval estimation

In this subsection, relying on the asymptotic normality of the MLEs, we construct ACIs for the unknown model parameters a, b, and θ. The same procedure is applied to obtain ACIs for the reliability indices under normal operating conditions. A prerequisite for constructing these intervals is the determination of the variance–covariance matrix of the estimators. Since obtaining the exact form of the Fisher information matrix is mathematically intractable in this case, it is approximated using the observed Fisher information matrix. The inverse of this matrix provides an estimate of the required variance–covariance matrix, which is given as follows:

$$\begin{aligned} \boldsymbol{I}^{-1}(\hat{\boldsymbol{\Psi}}) &= -\begin{bmatrix} \ell_{aa} & \ell_{ab} & \ell_{a\theta} \\ & \ell_{bb} & \ell_{b\theta} \\ & & \ell_{\theta\theta} \end{bmatrix}^{-1}_{\boldsymbol{\Psi}=\hat{\boldsymbol{\Psi}}} \\ &= \begin{bmatrix} \widehat{\mathrm{Var}}(\hat{a}) & \widehat{\mathrm{Cov}}(\hat{a},\hat{b}) & \widehat{\mathrm{Cov}}(\hat{a},\hat{\theta}) \\ & \widehat{\mathrm{Var}}(\hat{b}) & \widehat{\mathrm{Cov}}(\hat{b},\hat{\theta}) \\ & & \widehat{\mathrm{Var}}(\hat{\theta}) \end{bmatrix}, \end{aligned} \tag{10}$$

where $\hat{\boldsymbol{\Psi}} = (\hat{a}, \hat{b}, \hat{\theta})$, and

$$\ell_{aa} = \sum_{j=1}^{k}\left\{\sum_{i=1}^{r_j}\left\{\frac{\theta e^{a+bS_j}x_{ij}\left(1+x_{ij}\right)}{\left[\theta + e^{a+bS_j}x_{ij}\left(1+x_{ij}\right)\right]^2} - A_{ij}\right\} - (n_j - r_j)A_{r_j j}\right\},$$

$$\ell_{bb} = \sum_{j=1}^{k} S_j^2\left\{\sum_{i=1}^{r_j}\left\{\frac{\theta e^{a+bS_j}x_{ij}\left(1+x_{ij}\right)}{\left[\theta + e^{a+bS_j}x_{ij}\left(1+x_{ij}\right)\right]^2} - A_{ij}\right\} - (n_j - r_j)A_{r_j j}\right\},$$

$$\ell_{\theta\theta} = -\sum_{j=1}^{k}\sum_{i=1}^{r_j}\frac{1}{\left[\theta + e^{a+bS_j}x_{ij}\left(1+x_{ij}\right)\right]^2},$$

$$\ell_{ab} = \sum_{j=1}^{k} S_j\left\{\sum_{i=1}^{r_j}\left\{\frac{\theta e^{a+bS_j}x_{ij}\left(1+x_{ij}\right)}{\left[\theta + e^{a+bS_j}x_{ij}\left(1+x_{ij}\right)\right]^2} - A_{ij}\right\} - (n_j - r_j)A_{r_j j}\right\},$$

$$\ell_{a\theta} = -\sum_{j=1}^{k}\sum_{i=1}^{r_j}\left\{\frac{e^{a+bS_j}x_{ij}\left(1+x_{ij}\right)}{\left[\theta + e^{a+bS_j}x_{ij}\left(1+x_{ij}\right)\right]^2}\right\}$$

and

$$\ell_{b\theta} = -\sum_{j=1}^{k}\sum_{i=1}^{r_j} S_j\left\{\frac{e^{a+bS_j}x_{ij}\left(1+x_{ij}\right)}{\left[\theta + e^{a+bS_j}x_{ij}\left(1+x_{ij}\right)\right]^2}\right\}.$$

Accordingly, the $100(1-\tau)\%$ ACIs of the parameters a , b and θ are, respectively, given by

$$\hat{a} \pm z_{\tau/2}\sqrt{\widehat{\mathrm{Var}}(\hat{a})}, \quad \hat{b} \pm z_{\tau/2}\sqrt{\widehat{\mathrm{Var}}(\hat{b})} \text{ and } \hat{\theta} \pm z_{\tau/2}\sqrt{\widehat{\mathrm{Var}}(\hat{\theta})},$$

where $z_{\tau/2}$ denotes the upper $(\tau/2)$th percentile of the standard normal distribution.

Constructing ACIs for the RF and HRF under normal operating conditions constitutes an essential component of this study. To form these intervals, the delta method is employed to approximate the variances of the corresponding plug-in MLEs. In reliability settings, quantities such as the RF and HRF are typically nonlinear functions of the underlying model parameters, which makes exact analytical expressions for their variances difficult to derive. The delta method addresses this difficulty by linearizing the functions of interest around the parameter estimates, thereby providing a convenient large-sample variance approximation. Owing to its simplicity, computational efficiency, and solid theoretical foundation, the delta method is widely used in lifetime data analysis and ALTs. For further discussion of the delta method and related developments, see Ver Hoef [27] and Bera and Koley [28]. This framework provides a practical approach for quantifying the uncertainty in the estimated reliability measures. Let $\hat{\boldsymbol{\Delta}}_1$ denote the gradient vector of the RF with respect to the model parameters, evaluated at $\hat{\boldsymbol{\Psi}}$, and defined as

$$\hat{\boldsymbol{\Delta}}_1 = \left(\frac{\partial R_u}{\partial a}, \ \frac{\partial R_u}{\partial b}, \ \frac{\partial R_u}{\partial \theta}\right)\Bigg|_{\boldsymbol{\Psi}=\hat{\boldsymbol{\Psi}}},$$

where

$$\frac{\partial R_u}{\partial a} = -\frac{1}{2}t^2 e^{a+bS_u} R_u(t;\boldsymbol{\Psi}), \quad \frac{\partial R_u}{\partial b} = S_u \frac{\partial R_u}{\partial a}$$

and

$$\frac{\partial R_u}{\partial \theta} = -\log(1+t) R_u(t;\boldsymbol{\Psi}).$$

Thus, the approximate estimated variance of the MLE $\hat{R}_u(t)$ can be computed as

$$\widehat{\mathrm{Var}}(\hat{R}_u) \approx \left[\hat{\boldsymbol{\Delta}}_1 \boldsymbol{I}^{-1}(\hat{\boldsymbol{\Psi}})\hat{\boldsymbol{\Delta}}_1^{\top}\right], \tag{11}$$

where $\boldsymbol{I}^{-1}(\hat{\boldsymbol{\Psi}})$ is given by (10). Following that, the $100(1-\tau)\%$ ACI of the RF can be easily obtained as

$$\hat{R}_u(t) \pm z_{\tau/2}\sqrt{\widehat{\mathrm{Var}}(\hat{R}_u)}.$$

Likewise, the ACI for the HRF under normal operating conditions is obtained by using the delta method to approximate the variance of the corresponding estimator. Let $\hat{\boldsymbol{\Delta}}_2$ denote the gradient vector of the HRF with respect to the model parameters defined as

$$\hat{\boldsymbol{\Delta}}_2 = \left(\frac{\partial H_u}{\partial a}, \ \frac{\partial H_u}{\partial b}, \ \frac{\partial H_u}{\partial \theta}\right)\Bigg|_{\boldsymbol{\Psi}=\hat{\boldsymbol{\Psi}}},$$

where

$$\frac{\partial H_u}{\partial a} = te^{a+bS_u}, \ \frac{\partial H_u}{\partial b} = S_u \frac{\partial H_u}{\partial a}$$

and

$$\frac{\partial H_u}{\partial \theta} = \frac{1}{1+t}.$$

Thus, the approximate estimated variance of the MLE $\hat{H}_u(t)$ can be computed as

$$\widehat{\mathrm{Var}}(\hat{H}_u) \approx \left[\hat{\boldsymbol{\Delta}}_2 \boldsymbol{I}^{-1}(\hat{\boldsymbol{\Psi}})\hat{\boldsymbol{\Delta}}_2^{\top}\right]. \tag{12}$$

As a result, the $100(1-\tau)\%$ ACI of the HRF can be computed as follows

$$\hat{H}_u(t) \pm z_{\tau/2}\sqrt{\widehat{\mathrm{Var}}(\hat{H}_u)}.$$

4 Maximum Product of Spacings Estimation

In this section, we estimate the unknown parameters of the Hj distribution under CSALTs with Type-II censoring using the MPS method proposed by Cheng and Amin [29]. The MPS method is often preferable to maximum likelihood estimation when the likelihood function is difficult to handle numerically, for example, when it is highly nonlinear, multimodal, or prone to instability. The procedure maximizes the geometric mean of spacings formed by successive differences of the fitted cumulative probabilities corresponding to the ordered observations. The resulting estimators typically exhibit large-sample properties comparable to those of the MLEs. In particular, Cheng and Amin [29] established their consistency and asymptotic efficiency under mild conditions. Additional theoretical results, including asymptotic behavior and invariance properties, were reported by Ghosh and Jammalamadaka [30] and Anatolyev and Kosenok [31].

The robustness and flexibility of the MPS method have motivated its use in many statistical models; see, among others, Singh et al. [32], Almetwally et al. [33], and Du and Gui [34]. Here, we apply the MPS method to estimate the parameters a, b, and θ of the Hj distribution from Type-II censored CSALT data. Moreover, MPS-based estimators for the reliability measures under normal operating conditions are derived, and ACIs are constructed for all parameters and reliability quantities.

4.1 Point estimation

Let $x_{1j} < x_{2j} < \cdots < x_{r_j j}$, for $j = 1, 2, \ldots, k$, denote the ordered observed failure times from a Type-II censored sample at stress level S_j. Using (2), the spacing function for the parameters a, b, and θ, excluding the constant term, can be expressed as follows:

$$p(\mathbf{\Psi}) = \sum_{j=1}^{k} \sum_{i=1}^{r_j+1} \log(D_{ij}) - \sum_{j=1}^{k} (n_j - r_j) \Big[A_{r_j j} + \theta \log(1 + x_{r_j j}) \Big], \tag{13}$$

where $D_{ij} = B_{i^* j} - B_{ij}$, $i^* = i - 1$, and $B_{ij} = \frac{e^{-A_{ij}}}{(1+x_{ij})^{\theta}}$. It is clear that when $x_{0j} = 0$, we have $B_{0j} = 1$, and when $x_{r_j+1 j} = \infty$, we have $B_{r_j+1 j} = 0$. Consequently, the first and last spacings are given, respectively, by $D_{1j} = 1 - \frac{e^{-A_{1j}}}{(1+x_{1j})^{\theta}}$, and $D_{r_j+1 j} = \frac{e^{-A_{r_j j}}}{(1+x_{r_j j})^{\theta}}$.

The MPSEs of a, b and θ, say $\tilde{a}$, $\tilde{b}$ and $\tilde{\theta}$, can be obtained by solving the following three non-linear equations simultaneously

$$\frac{\partial p(\mathbf{\Psi})}{\partial a} = \sum_{j=1}^{k} \left[\sum_{i=1}^{r_j+1} \left(\frac{A_{ij} B_{ij} - A_{i^* j} B_{i^* j}}{D_{ij}} \right) - (n_j - r_j) A_{r_j j} \right] = 0, \tag{14}$$

$$\frac{\partial p(\mathbf{\Psi})}{\partial b} = \sum_{j=1}^{k} S_j \left[\sum_{i=1}^{r_j+1} \left(\frac{A_{ij} B_{ij} - A_{i^* j} B_{i^* j}}{D_{ij}} \right) - (n_j - r_j) A_{r_j j} \right] = 0 \tag{15}$$

and

$$\frac{\partial p(\mathbf{\Psi})}{\partial \theta} = \sum_{j=1}^{k} \left\{ \sum_{i=1}^{r_j+1} \left[\frac{B_{ij} \log\big(1 + x_{ij}\big) - B_{i^* j} \log\big(1 + x_{i^* j}\big)}{D_{ij}} \right] - (n_j - r_j) \log\Big(1 + x_{r_j j}\Big) \right\} = 0. \tag{16}$$

It is clear that the normal equations in (14)–(16) are nonlinear and contain complicated exponential terms. Hence, closed-form or explicit solutions for the MPSEs of a, b, and θ are not available, and the estimates must be obtained numerically. In practice, an iterative scheme such as the Newton–Raphson method can be used to solve the system simultaneously. To enhance convergence and numerical stability, suitable starting values are typically chosen, for instance, the corresponding MLEs. After obtaining the

MPSEs of a and b, the associated estimate of the scale parameter at stress level S_j follows from the invariance property as

$$\tilde{\lambda}_j = e^{\tilde{a}+\tilde{b}S_j}.$$

Let $\tilde{\lambda}_u = e^{\tilde{a}+\tilde{b}S_u}$ denote the MPSE of the scale parameter under the normal operating stress level S_u. Then, by the invariance property, the corresponding MPSEs of the RF and HRF at mission time t under S_u are given, respectively, by

$$\tilde{R}_u(t) = \frac{e^{-\frac{\tilde{\lambda}_u}{2}t^2}}{(1+t)^{\tilde{\theta}}}$$

and

$$\tilde{H}_u(t) = \tilde{\lambda}_u t + \frac{\tilde{\theta}}{1+t}.$$

4.2 Interval estimation

In this part, we construct ACIs for the parameters a, b, and θ, along with the reliability measures under normal operating conditions, by exploiting the asymptotic properties of the MPSEs. Because explicit closed-form expressions for the Fisher information matrix are typically unavailable under the MPS framework, we instead use the observed information matrix to estimate the required variances. The inverse of this matrix serves as an approximation to the variance–covariance matrix of the estimators and can be written as follows:

$$\begin{aligned} \boldsymbol{I}^{-1}(\tilde{\boldsymbol{\Psi}}) &= -\begin{bmatrix} p_{aa} & p_{ab} & p_{a\theta} \\ & p_{bb} & p_{b\theta} \\ & & p_{\theta\theta} \end{bmatrix}^{-1}_{\boldsymbol{\Psi}=\tilde{\boldsymbol{\Psi}}} \\ &= \begin{bmatrix} \widetilde{\mathrm{Var}}(\tilde{a}) & \widetilde{\mathrm{Cov}}(\tilde{a},\tilde{b}) & \widetilde{\mathrm{Cov}}(\tilde{a},\tilde{\theta}) \\ & \widetilde{\mathrm{Var}}(\tilde{b}) & \widetilde{\mathrm{Cov}}(\tilde{b},\tilde{\theta}) \\ & & \widetilde{\mathrm{Var}}(\tilde{\theta}) \end{bmatrix}, \end{aligned} \tag{17}$$

where $\tilde{\boldsymbol{\Psi}} = (\tilde{a},\tilde{b},\tilde{\theta})^\top$, and

$$p_{aa} = \sum_{j=1}^{k}\sum_{i=1}^{r_j+1} \frac{\left[A_{ij}B_{ij}(1-A_{ij}) - A_{i^*j}B_{i^*j}(1-A_{i^*j})\right]D_{ij} - \phi_{ij}^2}{D_{ij}^2} - \sum_{j=1}^{k}(n_j - r_j)A_{r_j j},$$

$$p_{bb} = \sum_{j=1}^{k}\sum_{i=1}^{r_j+1} S_j^2 \left\{\frac{\left[A_{ij}B_{ij}(1-A_{ij}) - A_{i^*j}B_{i^*j}(1-A_{i^*j})\right]D_{ij} - \phi_{ij}^2}{D_{ij}^2}\right\} - \sum_{j=1}^{k}(n_j - r_j)S_j^2 A_{r_j j},$$

$$p_{\theta\theta} = \sum_{j=1}^{k}\sum_{i=1}^{r_j+1} \frac{\left\{-B_{ij}\left[\log(1+x_{ij})\right]^2 + B_{i^*j}\left[\log(1+x_{i^*j})\right]^2\right\}D_{ij} - \varphi_{ij}^2}{D_{ij}^2},$$

$$p_{ab} = \sum_{j=1}^{k}\sum_{i=1}^{r_j+1} S_j \left\{\frac{\left[A_{ij}B_{ij}(1-A_{ij}) - A_{i^*j}B_{i^*j}(1-A_{i^*j})\right]D_{ij} - \phi_{ij}^2}{D_{ij}^2}\right\} - \sum_{j=1}^{k}(n_j - r_j)S_j A_{r_j j},$$

$$p_{a\theta} = \sum_{j=1}^{k}\sum_{i=1}^{r_j+1} \frac{\left[-A_{ij}B_{ij}\log(1+x_{ij}) + A_{i^*j}B_{i^*j}\log(1+x_{i^*j})\right]D_{ij} - \phi_{ij}\varphi_{ij}}{D_{ij}^2}$$

AdvantaCore Scientific Publishing

and

$$p_{b\theta} = \sum_{j=1}^{k}\sum_{i=1}^{r_j+1} S_j \left\{ \frac{\left[-A_{ij}B_{ij}\log(1+x_{ij}) + A_{i^*j}B_{i^*j}\log(1+x_{i^*j})\right] D_{ij} - \phi_{ij}\varphi_{ij}}{D_{ij}^2} \right\},$$

where $\phi_{ij} = A_{ij}B_{ij} - A_{i^*j}B_{i^*j}$, and $\varphi_{ij} = B_{ij}\log(1+x_{ij}) - B_{i^*j}\log(1+x_{i^*j})$. Then, the $100(1-\tau)\%$ ACIs of the parameters a , b and θ based on the MPSEs are, respectively, given by

$$\tilde{a} \pm z_{\tau/2}\sqrt{\widetilde{\mathrm{Var}}(\tilde{a})}, \quad \tilde{b} \pm z_{\tau/2}\sqrt{\widetilde{\mathrm{Var}}(\tilde{b})} \text{ and } \tilde{\theta} \pm z_{\tau/2}\sqrt{\widetilde{\mathrm{Var}}(\tilde{\theta})}.$$

On the other hand, the $100(1-\tau)\%$ ACIs for the RF and HRF under normal operating conditions can be obtained using the MPSEs as

$$\tilde{R}_u(t) \pm z_{\tau/2}\sqrt{\widetilde{\mathrm{Var}}(\tilde{R}_u)} \text{ and } \tilde{H}_u(t) \pm z_{\tau/2}\sqrt{\widetilde{\mathrm{Var}}(\tilde{H}_u)},$$

where $\widetilde{\mathrm{Var}}(\tilde{R}_u)$ and $\widetilde{\mathrm{Var}}(\tilde{H}_u)$ are obtained using the same expressions in (11) and (12), respectively, evaluated at the MPSEs of a, b and θ.

Remark. The ACIs derived in this study, based on both estimation methods, rely on the normal approximation of the estimators and the application of the delta method. Consequently, their accuracy may be affected in settings with small sample sizes or high levels of censoring, where the underlying asymptotic assumptions may not hold adequately. To mitigate this limitation, transformations of the model parameters may be considered. In particular, for strictly positive parameters, a logarithmic transformation can improve the normal approximation and lead to more stable interval estimation. However, the simulation results presented in this study indicate that the proposed confidence intervals perform satisfactorily under the considered sample sizes and censoring schemes, as evidenced by coverage percentages close to the nominal level.

5 Simulation Study

This section evaluates the performance of point and interval estimators according to established statistical criteria. The aim is to identify the most efficient method for estimating the model parameters and the reliability measures under normal operating conditions.

5.1 Simulation design

To conduct the simulation study, 1,000 Type-II censored CSALT samples were generated from the Hj distribution with true parameter values $a = 1$, $b = 5$, and $\theta = 2$. Three accelerated stress levels were considered, namely $S_1 = 0.25$, $S_2 = 0.5$, and $S_3 = 0.75$. Under normal operating conditions ($S_u = 0.1$) and mission time $t = 0.25$, the corresponding reliability measures are $R_u(t) = 0.56$ and $H_u(t) = 2.72$, with $\lambda_u = 4.48$. To investigate the effect of the effective sample size, different group sizes were considered at each stress level. The main simulation settings are summarized in Table 1.

Table 1: Summary of the simulation design.

General Settings	
Quantity	Value
True parameters	$a = 1, b = 5, \theta = 2$
Normal stress level	$S_u = 0.1$
Mission time	$t = 0.25$
$R_u(t)$	0.56
$H_u(t)$	2.72
λ_u	4.48

Table 1: Summary of the simulation design (continued).

General Settings		
Stress Levels and Censoring Scheme		
Stress level	Sample size n_i	Failures r_i (30%, 60%, 90%)
$S_1 = 0.25$	30	9, 18, 27
$S_2 = 0.50$	50	15, 30, 45
$S_3 = 0.75$	100	30, 60, 90

For the numerical implementation of the estimation procedures, the initial values required for the iterative optimization algorithms are chosen to be close to the true parameter values used in the simulation. This choice is intended to enhance numerical stability and ensure reliable convergence of both the maximum likelihood and MPS methods. Since the primary goal of the simulation study is to evaluate the performance of the estimators under the assumed model, rather than to assess sensitivity to initial values, this strategy provides a consistent and fair basis for comparison between the competing methods. To assess the maximization property of the obtained estimates, the profile log-likelihood functions for each model parameter are examined. The resulting curves exhibit unimodal behavior, indicating the presence of a unique dominant maximum. This provides strong evidence that the obtained estimates correspond to a unique dominant maximum of the likelihood function. For illustration, the corresponding profile log-likelihood plots are presented in the data analysis section. The same approach is followed for the MPSEs, where the profile log-spacing functions for each model parameter are examined, and similar unimodal behavior is observed. In addition, the optimization procedure is repeated using different initial values, and consistent estimates are obtained, confirming the stability and reliability of the estimation process. To assess the accuracy of the point estimators, two standard criteria were considered: Bias and the root mean square error (RMSE). Bias measures the average deviation of an estimator from the true parameter value, whereas RMSE reflects overall estimation accuracy. For the parameter θ, these measures are defined as

$$Bias = \frac{1}{1000}\sum_{i=1}^{1000}\left(\ddot{\theta}^{(i)} - \theta\right) \text{ and } RMSE = \sqrt{\frac{1}{1000}\sum_{i=1}^{1000}\left(\ddot{\theta}^{(i)} - \theta\right)^2},$$

respectively, where $\ddot{\theta}^{(i)}$ denotes the estimate of θ obtained from the ith simulated sample using either the MLE or MPSE method, and θ denotes the true value. The Bias and RMSE for the remaining parameters are computed similarly. When comparing the two estimation methods, the estimator with smaller Bias and RMSE values is regarded as more efficient. The simulation results based on these criteria are summarized in Tables 2–7.

The accuracy of the ACIs is assessed using two main criteria: the average interval length (AIL) and the coverage probability (CP). The AIL reflects estimation precision, where shorter intervals indicate higher precision, whereas the CP measures how often the confidence interval contains the true parameter value. For the parameter θ, the AIL and CP are defined as

$$AIL = \frac{1}{1000}\sum_{i=1}^{1000}(U_i - L_i) \text{ and } CP = \frac{1}{1000}\sum_{i=1}^{1000}\mathbb{I}_{(L_i,U_i)}(\theta), \tag{18}$$

respectively, where L_i and U_i are the lower and upper limits of the confidence interval for the ith simulated sample, computed using either the MLE or MPSE method. The indicator function $\mathbb{I}(\cdot)$ takes the value one if the true parameter value θ lies within the interval and zero otherwise. The AIL and CP for the remaining parameters are obtained similarly. When comparing the two methods, preference is given to the approach that yields smaller AIL values while keeping the CP close to the nominal 95% level. The simulation results for the AIL and CP are reported in Tables 2–7.

5.2 Simulation outcomes

The results presented in Tables 2–7 lead to the following conclusions:

1. The MLEs outperform the MPSEs in terms of RMSE when estimating the parameters a, b, and θ. As shown in Tables 2–4, the RMSE values obtained using the MLEs are consistently smaller than those of the MPSEs, indicating that the MLEs provide more efficient estimates for these parameters.
2. Under normal operating conditions, the MPSEs perform better than the MLEs in terms of RMSE for estimating λ_u, the RF, and the HRF. As presented in Tables 5–7, the MPSEs produce lower RMSE values for these quantities.
3. All estimates demonstrate consistency. The results indicate that, as the sample size increases, the RMSE values decrease, confirming an inverse relationship between RMSE and sample size. This finding implies that both estimation methods yield consistent estimators.
4. The MLEs exhibit superior performance in terms of bias when estimating the parameters a, b, and θ. Tables 2–4 reveal that the bias values for the MLEs are smaller than those for the MPSEs, suggesting that the MLEs tend to be closer to the true parameter values.
5. Under normal operating conditions, for λ_u and the HRF, the MPSEs also outperform the MLEs in terms of bias. Tables 5 and 7 show that the MPSEs yield lower bias values than the MLEs. Conversely, Table 6 shows that, for the RF, the MLEs yield lower bias values, indicating better performance in this case.
6. The ACIs based on the MLEs exhibit superior performance compared to those obtained using the MPSEs in terms of AIL when estimating the parameters a, b, and θ. Tables 2–4 clearly show the superiority of the MLE-based ACIs over the MPSE-based ones for these parameters.
7. Under normal operating conditions, the ACIs based on the MPSEs produce shorter AILs for λ_u, the RF, and the HRF. Tables 5–7 clearly demonstrate the superiority of the MPSE-based ACIs over the MLE-based ones for these quantities.
8. Tables 2–4 indicate that the ACIs obtained using the MPSEs yield higher CPs than those derived from the MLEs for the parameters a, b, and θ. For parameter a, the MPSE-based ACIs achieve CPs ranging from 0.953 to 0.986, whereas the MLE-based ACIs range from 0.855 to 0.949. A similar pattern is observed for the parameters b and θ.
9. Under normal operating conditions, the ACIs obtained using the MLEs outperform those based on the MPSEs in terms of CPs for λ_u and the HRF, whereas the MPSE-based ACIs achieve higher CPs for the RF. Tables 5 and 7 show that the MLE-based ACIs provide CPs ranging from 0.844 to 0.973 for λ_u, compared to 0.743–0.879 for the MPSE-based ACIs, indicating better coverage performance. A similar trend is observed for the HRF. In contrast, Table 6 shows that the MPSE-based ACIs yield higher CPs for the RF, ranging from 0.891 to 0.966, while the MLE-based ACIs range from 0.909 to 0.957.
10. In all cases, as the number of observations increases, the CPs approach the nominal 95% confidence level, confirming the asymptotic validity of both estimation procedures. Furthermore, for interval estimation of the RF and HRF, the ACIs based on the MPSEs generally yield shorter AILs. Additionally, the intervals obtained using the MLEs typically achieve higher CPs for the HRF, while those based on the MPSEs tend to achieve higher CPs for the RF. This indicates that the superiority of each method depends on the reliability measure being estimated.
11. The simulation results indicate that increasing the number of observations improves the overall performance of the estimation procedures. This improvement is reflected in both point and interval estimation results. Overall, the most favorable results are obtained for the largest combination of observations, $(r_1, r_2, r_3) = (27, 45, 90)$.

Overall, the simulation results indicate that the MLEs generally outperform the MPSEs in estimating the model parameters a, b, and θ. Under normal operating conditions, however, the MPSEs generally outperform the MLEs in estimating the scale parameter λ_u and the reliability measures. In addition, the results show that increasing the number of observations generally improves the performance of the estimation procedures. These findings confirm the effectiveness of the proposed estimation methods under the considered Type-II censored CSALT scheme.

Table 2: The point estimation results of a.

r_1	r_2	r_3	MLE					MPSE				
			Estimate	RMSE	Bias	AIL	CP	Estimate	RMSE	Bias	AIL	CP
		30	0.63844	5.37393	-0.36156	247.539	85.5164	-2.20135	11.2240	-3.20135	309.971	96.2810
	15	60	0.54691	6.07257	-0.45309	294.863	86.0879	-1.60071	9.16741	-2.60071	107.001	96.2551
		90	-0.10638	6.71029	-1.10638	199.281	89.8045	-1.69500	9.12499	-2.69500	169.144	96.5447
		30	1.02459	1.13138	0.02459	4.13249	91.6331	0.53356	1.70091	-0.46644	4.89259	96.1962
9	30	60	1.07038	1.05875	0.07038	3.97357	91.5408	0.57573	1.22724	-0.42427	4.78075	97.6000
		90	0.96992	1.01539	-0.03008	3.98490	93.9068	0.54793	1.22224	-0.45207	4.65725	96.8000
		30	1.01782	0.85193	0.01782	3.21321	92.9930	0.75277	0.91651	-0.24723	3.48942	95.3000
	45	60	1.02212	0.77487	0.02212	2.92046	92.9969	0.72341	0.84377	-0.27659	3.16813	95.6000
		90	1.03704	0.74163	0.03704	2.82088	92.4820	0.72894	0.80916	-0.27106	3.07247	96.4000
		30	-0.03379	8.47392	-1.03379	621.480	89.4550	-2.93936	13.8021	-3.93936	292.590	97.1728
	15	60	0.27776	7.00778	-0.72224	402.193	89.5016	-1.86876	10.0901	-2.86876	246.722	97.1545
		90	0.12612	7.37832	-0.87388	190.496	91.1085	-1.92837	10.5497	-2.92837	126.804	97.0528
		30	1.01119	0.90206	0.01119	3.29132	92.6349	0.29769	3.46087	-0.70231	13.7881	97.5806
18	30	60	1.04533	0.86162	0.04533	3.22473	91.1021	0.54550	1.11330	-0.45450	4.10419	98.3000
		90	1.04358	0.90992	0.04358	3.17902	91.2698	0.53647	1.15418	-0.46353	4.07699	97.3000
		30	0.99218	0.71281	-0.00782	2.71817	94.0000	0.69041	0.81128	-0.30959	3.05441	95.9000
	45	60	1.03201	0.67804	0.03201	2.54027	93.5549	0.69118	0.78760	-0.30882	2.87503	96.8000
		90	1.04886	0.66604	0.04886	2.47345	92.6559	0.70281	0.76642	-0.29719	2.80429	96.3000
		30	1.01383	3.03605	0.01383	2.98089	93.4322	-0.39783	6.38310	-1.39783	94.0583	98.6829
	15	60	0.95902	2.60948	-0.04098	35.5453	90.4311	-0.02345	5.47346	-1.02345	83.0611	97.1689
		90	1.01657	1.54146	0.01657	30.2822	91.7548	0.34553	3.42537	-0.65447	10.5284	97.6931
		30	1.03738	0.61070	0.03738	2.33758	94.2564	0.54174	1.65321	-0.45826	9.82577	98.3968
27	30	60	1.04784	0.61669	0.04784	2.28958	91.1366	0.55686	1.88649	-0.44314	4.65035	97.4975
		90	1.02036	0.59965	0.02036	2.29836	92.8279	0.59475	0.90022	-0.40525	3.05634	98.2000
		30	1.01288	0.55803	0.01288	2.14227	94.8898	0.72465	0.67200	-0.27535	2.46480	97.5000
	45	60	1.02869	0.54174	0.02869	2.03984	93.3673	0.69198	0.68468	-0.30802	2.37598	96.4000
		90	1.01481	0.52091	0.01481	2.00403	93.6000	0.68703	0.65664	-0.31297	2.32701	96.6000

Table 3: The estimation results of b.

r_1	r_2	r_3	MLE					MPSE				
			Estimate	RMSE	Bias	AIL	CP	Estimate	RMSE	Bias	AIL	CP
		30	5.43062	7.35198	0.43062	334.915	88.0051	8.76811	14.8514	3.76811	382.090	96.4398
	15	60	5.63807	8.06332	0.63807	393.006	87.8661	8.39105	12.1590	3.39105	142.467	96.3563
		90	6.49785	8.91509	1.49785	265.562	90.7821	8.53278	12.1147	3.53278	225.363	96.4431
		30	5.01818	1.69609	0.01818	6.05660	93.1452	5.53264	2.38771	0.53264	7.07710	96.0961
9	30	60	4.93108	1.44141	-0.06892	5.39197	92.3464	5.50076	1.64128	0.50076	6.43872	97.6000
		90	5.05307	1.35887	0.05307	5.31796	93.3094	5.55070	1.60400	0.55070	6.19725	96.5000
		30	5.01948	1.39660	0.01948	5.18615	92.8929	5.25274	1.50631	0.25274	5.62767	94.4000
	45	60	4.98668	1.10531	-0.01332	4.19905	94.1298	5.30780	1.17881	0.30780	4.52801	95.3000
		90	4.96794	1.02885	-0.03206	3.90377	93.0999	5.31289	1.10348	0.31289	4.23172	96.5000
		30	6.22983	11.1397	1.22983	802.983	92.4641	9.04027	18.0142	4.04027	302.652	97.3713
	15	60	5.98714	9.31648	0.98714	536.167	91.1983	8.73992	13.3843	3.73992	328.801	97.0528
		90	6.19017	9.80808	1.19017	253.895	92.1478	8.83911	14.0124	3.83911	168.933	96.5447

Table 3: The estimation results of b (continued).

r_1	r_2	r_3	MLE					MPSE				
			Estimate	RMSE	Bias	AIL	CP	Estimate	RMSE	Bias	AIL	CP
		30	5.03793	1.31882	0.03793	4.84233	94.5021	5.77831	4.53841	0.77831	6.01230	96.5622
18	30	60	4.96416	1.16619	-0.03584	4.36644	93.1244	5.53348	1.46613	0.53348	5.49473	97.8000
		90	4.96742	1.20228	-0.03258	4.23400	91.9501	5.55999	1.50067	0.55999	5.39909	96.8000
		30	5.06291	1.15322	0.06291	4.37476	95.2000	5.34810	1.26164	0.34810	4.87204	95.9000
	45	60	4.97683	0.96307	-0.02317	3.63798	94.6626	5.34857	1.08315	0.34857	4.07611	96.4000
		90	4.95498	0.91762	-0.04502	3.40844	93.3602	5.34439	1.03274	0.34439	3.83726	96.1000
		30	5.03009	4.04317	0.03009	3.63386	95.2331	6.43478	8.29112	1.43478	164.077	97.7436
	15	60	5.07864	3.48259	0.07864	47.4392	92.7445	6.28140	7.27061	1.28140	110.732	96.5622
		90	4.99560	2.04587	-0.00440	40.3608	93.2347	5.80797	4.53758	0.80797	13.9801	97.4925
		30	4.99749	0.94416	-0.00251	3.67146	95.4872	5.37846	1.93408	0.37846	36.0291	97.2864
27	30	60	4.95405	0.85615	-0.04595	3.18135	92.2836	5.51067	2.51323	0.51067	6.27768	96.7968
		90	4.98940	0.79725	-0.01060	3.09660	94.2623	5.47641	1.15902	0.47641	4.06917	97.6000
		30	5.02506	0.94032	0.02506	3.59028	95.6914	5.28323	1.05725	0.28323	4.06303	96.5000
	45	60	4.97629	0.78790	-0.02371	2.97723	93.9796	5.33948	0.94091	0.33948	3.40652	95.6000
		90	4.99938	0.72312	-0.00062	2.78824	94.7000	5.36012	0.87233	0.36012	3.19855	95.8000

Table 4: The estimation results of θ.

r_1	r_2	r_3	MLE					MPSE				
			Estimate	RMSE	Bias	AIL	CP	Estimate	RMSE	Bias	AIL	CP
		30	1.76132	0.83261	-0.23868	2.95763	90.9548	2.31152	0.81436	0.31152	3.05111	92.9719
	15	60	1.84273	0.77632	-0.15727	2.89908	90.9091	2.29900	0.75184	0.29900	2.95952	95.0000
		90	1.93516	0.77633	-0.06484	2.82483	91.7942	2.26418	0.73273	0.26418	2.83619	94.0000
		30	1.87445	0.74958	-0.12555	2.72243	93.3468	2.24128	0.73543	0.24128	2.79387	95.9000
9	30	60	1.90680	0.72636	-0.09320	2.68524	93.0514	2.26373	0.71676	0.26373	2.73528	95.5000
		90	1.90396	0.69914	-0.09604	2.61471	92.8315	2.22776	0.69136	0.22776	2.64853	95.8000
		30	1.91040	0.68993	-0.08960	2.53961	93.3934	2.21870	0.68699	0.21870	2.58248	95.9000
	45	60	1.96235	0.68092	-0.03765	2.52641	92.5850	2.25319	0.68814	0.25319	2.55397	95.2000
		90	1.90266	0.64300	-0.09734	2.45784	92.9969	2.21072	0.65066	0.21072	2.48812	95.8000
		30	1.77298	0.80380	-0.22702	2.76023	88.1733	2.38226	0.90585	0.38226	2.88221	86.6062
	15	60	1.87943	0.74662	-0.12057	2.73665	90.3805	2.32123	0.77750	0.32123	2.81980	90.4000
		90	1.88100	0.71553	-0.11900	2.64285	90.3559	2.28007	0.73653	0.28007	2.72366	91.5000
		30	1.85852	0.72845	-0.14148	2.66459	93.2573	2.27531	0.74941	0.27531	2.74499	94.1767
18	30	60	1.91126	0.70838	-0.08874	2.63331	92.6188	2.29340	0.72503	0.29340	2.69584	94.2000
		90	1.85900	0.69976	-0.14100	2.54773	91.4966	2.25679	0.69190	0.25679	2.62055	94.9000
		30	1.89992	0.67520	-0.10008	2.48009	93.1000	2.23058	0.67057	0.23058	2.51493	95.3000
	45	60	1.94133	0.66302	-0.05867	2.47626	92.1450	2.27033	0.67543	0.27033	2.50531	95.0000
		90	1.90255	0.64295	-0.09745	2.42895	93.0584	2.23343	0.64435	0.23343	2.45520	95.2000
		30	1.81145	0.70014	-0.18855	2.60271	91.3228	2.29186	0.80211	0.29186	2.69330	93.2798
	15	60	1.90299	0.67121	-0.09701	2.53584	92.3239	2.29291	0.72687	0.29291	2.61212	93.8939
		90	1.87702	0.65740	-0.12298	2.44943	92.8118	2.25902	0.68784	0.25902	2.53812	94.6000
		30	1.86518	0.69172	-0.13482	2.56985	93.0256	2.28550	0.76333	0.28550	2.66663	94.7000
27	30	60	1.92253	0.65886	-0.07747	2.51718	93.4307	2.30594	0.72457	0.30594	2.60250	94.3000
		90	1.90545	0.65426	-0.09455	2.44766	92.5205	2.28002	0.69842	0.28002	2.53001	94.2000

Table 4: The estimation results of θ (continued).

r_1	r_2	r_3	MLE					MPSE				
			Estimate	RMSE	Bias	AIL	CP	Estimate	RMSE	Bias	AIL	CP
		30	1.90171	0.66537	-0.09829	2.44730	92.6854	2.24871	0.68103	0.24871	2.50299	95.0000
	45	60	1.94512	0.65117	-0.05488	2.43235	92.9592	2.29523	0.68948	0.29523	2.48467	94.4000
		90	1.92441	0.63151	-0.07559	2.37981	93.2000	2.26320	0.66264	0.26320	2.42624	94.2000

Table 5: The estimation results of λ_u.

r_1	r_2	r_3	MLE					MPSE				
			Estimate	RMSE	Bias	AIL	CP	Estimate	RMSE	Bias	AIL	CP
		30	499.751	13791.3	495.269	960216	90.9320	459.661	14340.4	455.179	186428	74.3034
	15	60	9.99838	13.5830	5.51669	27.5070	89.4351	5.10022	8.29845	0.61853	17.2469	76.8219
		90	7.78812	10.4364	3.30643	22.0985	84.4972	5.00230	7.20779	0.52061	16.6721	74.5935
		30	7.02579	9.69105	2.54410	17.9743	89.3145	4.91891	7.44144	0.43723	14.2952	81.6817
9	30	60	6.80256	6.29033	2.32087	16.4830	90.8359	4.59074	4.17851	0.10905	12.2067	81.8000
		90	6.08113	5.50930	1.59944	14.7800	90.2031	4.54198	4.49822	0.06029	11.8788	82.6000
		30	5.92583	6.13547	1.44414	13.7919	90.5906	5.08248	14.6462	0.60080	13.2159	84.9000
	45	60	5.64767	4.07236	1.16598	12.0900	90.3193	4.37892	3.13463	-0.10277	9.86225	84.5000
		90	5.63677	3.83038	1.15508	11.9198	91.5551	4.33782	2.91537	-0.14387	9.67286	84.6000
		30	7.07802	6.25824	2.59633	15.7529	94.9052	3.97540	4.39010	-0.50629	11.0355	82.4268
	15	60	6.63252	5.17609	2.15083	15.0326	94.3796	4.03044	3.66800	-0.45125	10.9529	82.0122
		90	6.25550	5.00685	1.77381	14.2637	92.6097	4.21658	4.23135	-0.26511	11.1982	82.2154
		30	5.83704	4.41341	1.35535	12.3422	92.4274	4.06419	3.40306	-0.41750	9.75113	82.8456
18	30	60	5.87253	4.03177	1.39084	12.3356	92.7199	4.05555	2.96589	-0.42614	9.59729	82.8000
		90	5.95422	4.10510	1.47253	12.3405	91.8367	4.12915	3.34101	-0.35254	9.66524	82.9000
		30	5.32931	3.48940	0.84762	10.6015	92.8000	4.13098	2.80474	-0.35070	8.91310	86.2000
	45	60	5.39880	3.19240	0.91711	10.3243	92.4471	4.06978	2.48895	-0.41191	8.46931	85.6000
		90	5.47491	3.30337	0.99322	10.3393	92.9577	4.10517	2.53820	-0.37652	8.46274	83.8000
		30	5.58508	2.93732	1.10339	10.0727	97.3517	3.87769	2.39338	-0.60400	8.19305	87.9433
	15	60	5.61158	3.26396	1.12989	10.1510	95.1630	3.93833	2.58247	-0.54336	8.30250	87.5632
		90	5.43162	3.05140	0.94993	9.83768	95.3488	3.83577	2.44483	-0.64592	8.08625	86.3591
		30	5.26343	2.67695	0.78174	9.18654	94.7692	3.88860	2.25166	-0.59308	7.74927	84.8697
27	30	60	5.33957	2.86894	0.85788	9.26572	93.4307	3.88343	2.34203	-0.59826	7.69272	84.9850
		90	5.19230	2.74249	0.71061	8.99859	94.8770	3.77817	2.28463	-0.70352	7.48535	85.3000
		30	5.05337	2.37029	0.57168	8.45303	94.1884	3.96337	2.01253	-0.51831	7.36326	85.4000
	45	60	5.10393	2.42877	0.62224	8.26503	93.3673	3.87403	2.04754	-0.60766	7.01424	84.1000
		90	5.02042	2.34794	0.53873	8.06153	94.6000	3.82578	1.99906	-0.65591	6.87238	85.1000

Table 6: The estimation results of $R(t)$.

r_1	r_2	r_3	MLE					MPSE				
			Estimate	RMSE	Bias	AIL	CP	Estimate	RMSE	Bias	AIL	CP
		30	0.51014	0.13940	-0.04622	0.42543	92.7136	0.52190	0.10794	-0.03446	0.36930	94.7791
	15	60	0.50723	0.12958	-0.04913	0.41305	94.4619	0.52272	0.09977	-0.03364	0.35981	96.6000
		90	0.52505	0.11498	-0.03131	0.37700	93.4631	0.52619	0.09671	-0.03017	0.35383	96.1000

Table 6: The estimation results of $R(t)$ (continued).

r_1	r_2	r_3	MLE					MPSE				
			Estimate	RMSE	Bias	AIL	CP	Estimate	RMSE	Bias	AIL	CP
		30	0.54253	0.09997	-0.01383	0.36191	95.4637	0.53103	0.09114	-0.02533	0.33604	96.2000
9	30	60	0.53673	0.09136	-0.01963	0.33393	95.3676	0.52889	0.08209	-0.02747	0.30901	96.2000
		90	0.54788	0.08506	-0.00848	0.31097	93.4289	0.53387	0.08040	-0.02249	0.29595	94.5000
		30	0.55237	0.09108	-0.00399	0.34434	95.7958	0.53465	0.08727	-0.02171	0.32701	95.9000
	45	60	0.54725	0.08142	-0.00911	0.30647	95.0566	0.53278	0.07740	-0.02358	0.29218	94.8000
		90	0.55380	0.07631	-0.00256	0.29185	93.5118	0.53801	0.07327	-0.01835	0.27869	93.8000
		30	0.54881	0.09348	-0.00755	0.30958	90.9836	0.52606	0.08742	-0.03030	0.28829	89.1239
	15	60	0.54049	0.08099	-0.01587	0.29478	94.3975	0.52986	0.07430	-0.02650	0.28041	94.6000
		90	0.54655	0.07889	-0.00981	0.28552	93.3410	0.53211	0.07512	-0.02425	0.27495	94.5000
		30	0.55707	0.08307	0.00071	0.30198	93.7759	0.53558	0.07732	-0.02078	0.28855	94.1767
18	30	60	0.54853	0.07508	-0.00783	0.28078	95.2477	0.53228	0.07074	-0.02408	0.26969	94.9000
		90	0.55343	0.07426	-0.00292	0.27137	93.3107	0.53566	0.07085	-0.02070	0.26108	93.8000
		30	0.56011	0.08005	0.00375	0.29604	93.9000	0.53940	0.07439	-0.01696	0.28397	94.7000
	45	60	0.55261	0.07268	-0.00375	0.27405	95.0655	0.53467	0.06926	-0.02169	0.26398	94.3000
		90	0.55597	0.07181	-0.00039	0.26342	92.8571	0.53840	0.06764	-0.01796	0.25459	93.5000
		30	0.56602	0.07762	0.00966	0.28761	92.5926	0.53661	0.07680	-0.01975	0.27663	91.3741
	15	60	0.55347	0.07135	-0.00289	0.26996	93.7960	0.53423	0.06989	-0.02213	0.26219	92.6927
		90	0.55953	0.06983	0.00317	0.26066	93.2347	0.53971	0.06654	-0.01664	0.25474	93.5000
		30	0.56474	0.07626	0.00838	0.28681	93.3333	0.53678	0.07440	-0.01958	0.27784	92.9000
27	30	60	0.55551	0.07002	-0.00085	0.26757	94.6820	0.53347	0.06919	-0.02289	0.26087	93.3000
		90	0.55999	0.06870	0.00363	0.25714	93.1352	0.53813	0.06662	-0.01823	0.25204	94.0000
		30	0.56377	0.07543	0.00741	0.28303	92.9860	0.53941	0.07079	-0.01695	0.27331	94.1000
	45	60	0.55681	0.07031	0.00045	0.26540	94.3878	0.53473	0.06776	-0.02163	0.25779	93.1000
		90	0.56055	0.06825	0.00419	0.25535	92.6000	0.53920	0.06532	-0.01716	0.24911	93.8000

Table 7: The estimation results of $H(t)$.

r_1	r_2	r_3	MLE					MPSE				
			Estimate	RMSE	Bias	AIL	CP	Estimate	RMSE	Bias	AIL	CP
		30	126.347	3447.91	123.626	239451	95.4774	116.764	3585.18	114.044	45344.5	93.0723
	15	60	3.97378	3.19088	1.25336	7.41989	96.7607	3.11425	1.99494	0.39383	5.14018	93.8000
		90	3.49516	2.39408	0.77474	6.08117	94.1586	3.06192	1.68367	0.34150	4.95514	92.9000
		30	3.25601	2.38886	0.53558	4.97950	95.4637	3.02276	1.91219	0.30233	4.29075	94.8000
9	30	60	3.22608	1.42268	0.50565	4.37685	95.2669	2.95867	1.00691	0.23825	3.55004	95.3000
		90	3.04345	1.22152	0.32303	3.85706	94.7431	2.91771	1.04717	0.19728	3.37135	94.7000
		30	3.00978	1.56184	0.28936	3.97526	95.0951	3.04558	3.75551	0.32516	4.02657	95.6000
	45	60	2.98180	0.95683	0.26138	3.22340	95.8805	2.89728	0.79814	0.17686	2.86613	96.2000
		90	2.93132	0.87042	0.21090	3.03424	95.5716	2.85304	0.73360	0.13261	2.68806	95.5000
		30	3.18789	1.39327	0.46747	3.76034	95.6674	2.89966	0.99277	0.17924	3.01352	95.0655
	15	60	3.16167	1.09830	0.44125	3.59217	97.6744	2.86460	0.77100	0.14417	2.94960	96.9000
		90	3.06867	1.07804	0.34825	3.40890	96.2113	2.87820	0.92639	0.15778	2.98290	94.7000
		30	2.94607	0.99260	0.22565	3.08890	95.1245	2.83629	0.80020	0.11587	2.72006	95.6827
18	30	60	2.99714	0.85813	0.27672	2.91363	96.2588	2.84860	0.65307	0.12818	2.52463	96.7000
		90	2.97575	0.86378	0.25533	2.85833	95.8050	2.83772	0.75060	0.11730	2.47734	95.5000

Table 7: The estimation results of $H(t)$ (continued).

r_1	r_2	r_3	MLE					MPSE				
			Estimate	RMSE	Bias	AIL	CP	Estimate	RMSE	Bias	AIL	CP
		30	2.85226	0.84392	0.13184	2.81529	94.3000	2.81721	0.72862	0.09679	2.59347	95.9000
	45	60	2.90276	0.72561	0.18234	2.53855	96.2739	2.83371	0.60477	0.11329	2.29070	96.7000
		90	2.89077	0.74637	0.17035	2.44612	95.1710	2.81304	0.61605	0.09261	2.19447	95.5000
		30	2.84543	0.69123	0.12500	2.43756	95.7672	2.80291	0.59347	0.08249	2.23722	95.3862
	15	60	2.92528	0.71373	0.20486	2.38666	97.1609	2.81891	0.57632	0.09848	2.15748	96.7968
		90	2.85952	0.66463	0.13909	2.28401	95.5603	2.76615	0.54211	0.04573	2.07222	96.0000
		30	2.80800	0.64435	0.08758	2.34188	95.7949	2.80055	0.57088	0.08013	2.19388	96.3000
27	30	60	2.87291	0.63714	0.15249	2.21891	96.7675	2.81561	0.53195	0.09518	2.03884	97.2000
		90	2.82243	0.60360	0.10201	2.10477	95.3893	2.76856	0.50839	0.04814	1.93786	95.6000
		30	2.78471	0.61832	0.06429	2.30367	95.2906	2.78981	0.55372	0.06939	2.17967	97.3000
	45	60	2.83208	0.57690	0.11166	2.10696	96.0204	2.80469	0.50122	0.08427	1.96509	97.2000
		90	2.79463	0.55535	0.07421	1.98788	94.9000	2.76700	0.48313	0.04658	1.85590	95.5000

6 Application

This section evaluates the practical applicability of the proposed methodology using a real accelerated life test dataset. The data, reported by Stone [35], consist of observations on insulation materials subjected to different voltage stress levels. In this study, we focus on the results obtained at 52.5 kV and 55 kV. For convenience, the recorded lifetimes are rescaled by dividing all observations by 2000. The transformed data for each stress level are presented in Table 8.

Table 8: Failure times of steel specimens.

Stress (s)	Failure times									
52.5 kV	0.1225	0.123	0.175	0.275	0.300	0.370	0.3725	0.505	0.595	0.6125
	0.695	0.729	0.740	0.754	0.845	1.225	1.500	2.345	3.0475	3.100
55 kV	0.057	0.066	0.072	0.081	0.111	0.129	0.149	0.150	0.156	0.198
	0.222	0.260	0.3725	0.386	0.620	0.633	0.732	0.870	1.220	1.300

The MLEs and MPSEs along with their standard errors (SEs) for the dataset in 8 are reported in Table 9. To assess the adequacy of the Hj model under the two stress levels, the Kolmogorov–Smirnov (KS) goodness-of-fit test is employed. As shown in Table 9, the corresponding p-values exceed 0.05 for both stress levels, indicating that the null hypothesis of distributional adequacy cannot be rejected. These results suggest that the Hj distribution provides a satisfactory fit to the data and is appropriate for subsequent inference under the considered stress conditions.

Figure 1 presents violin plots of the observed failure times under the two stress levels, 52.5 kV and 55 kV. Each violin plot combines a kernel density estimate with a boxplot, providing a comprehensive visualization of the distribution, including its spread, central tendency, and potential skewness. The embedded boxplots display the median and interquartile range for each stress level. The results reveal clear differences in the distribution of failure times across the two stress levels. At the lower stress level (52.5 kV), the distribution exhibits a wider spread with a longer upper tail. In contrast, the higher stress level (55 kV) shows a more concentrated distribution, with failure times clustered closer to smaller values and reduced variability. The P–P plots for the dataset are presented in Figure 2, while the corresponding Q–Q plots are shown in Figure 3. In addition, Figure 4 provides a comparison between the theoretical and empirical RFs. These graphical diagnostics collectively demonstrate a close agreement between the fitted

model and the observed data, thereby supporting the adequacy of the Hj distribution for modeling the dataset. This conclusion is consistent with the numerical results reported in Table 9.

Table 9: The estimates, SE, and KS for both methods applied to the real dataset.

Stress	MLE						MPSE					
	λ	SE(λ)	θ	SE(θ)	KS	p-value	λ	SE(λ)	θ	SE(θ)	KS	p-value
52.5 kV	0.353	0.258	1.250	0.447	0.160	0.628	0.190	0.205	1.365	0.431	0.155	0.667
55 kV	1.433	1.409	2.661	0.897	0.139	0.784	0.569	1.165	2.857	0.877	0.147	0.725

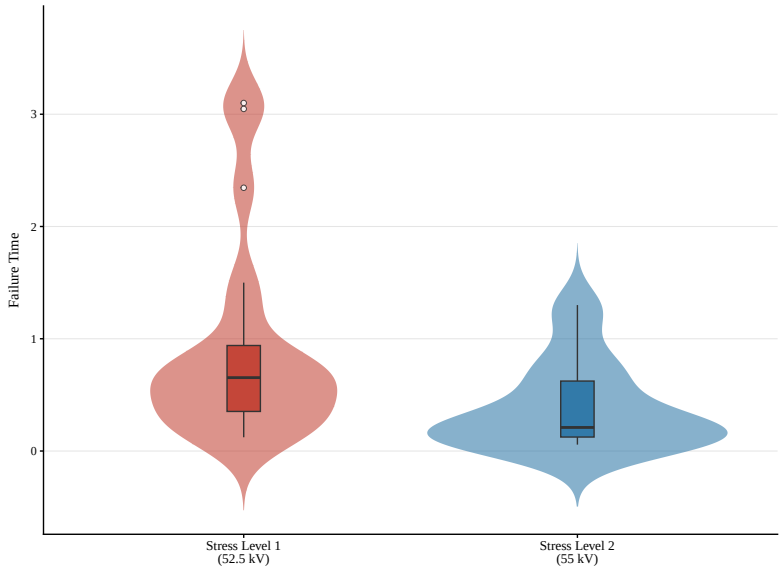

Figure 1: Violin plots of the observed failure times under two stress levels (52.5 kV and 55 kV).

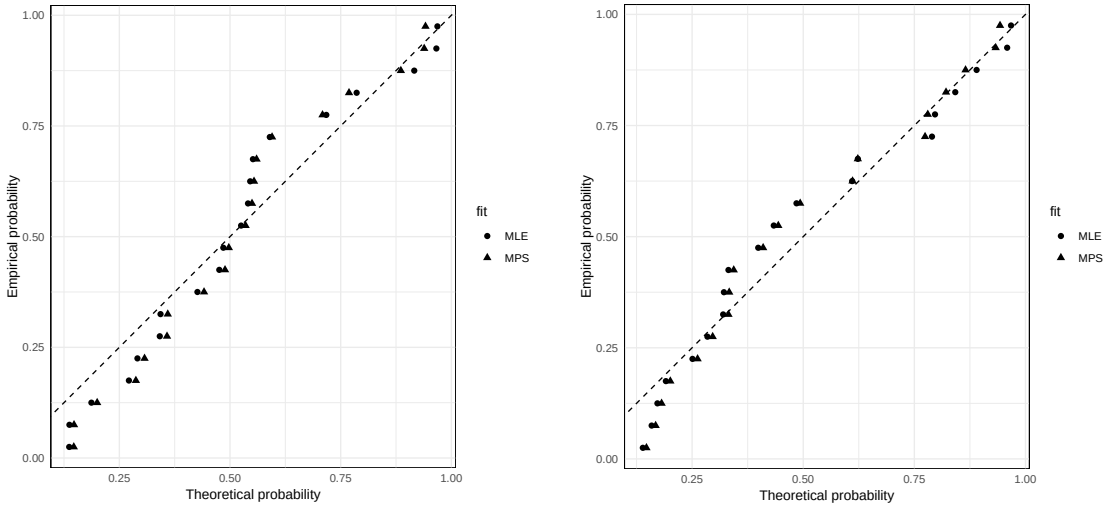

52.5kV 55kV

Figure 2: P–P plots for the real dataset at stress levels 52.5kV and 55kV.

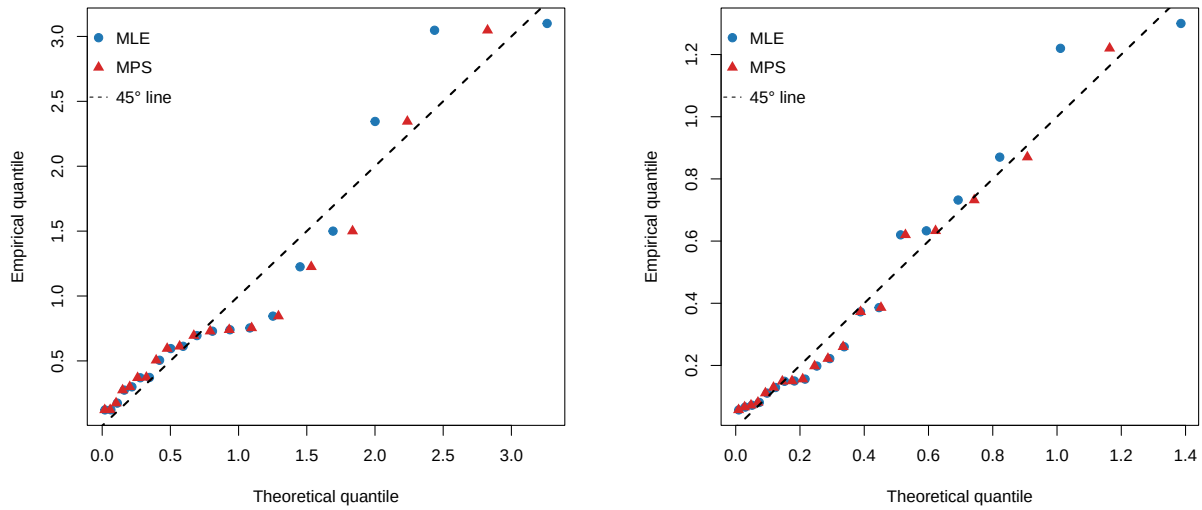

52.5kV 55kV

Figure 3: Q-Q plots for the real dataset at stress levels 52.5kV and 55kV.

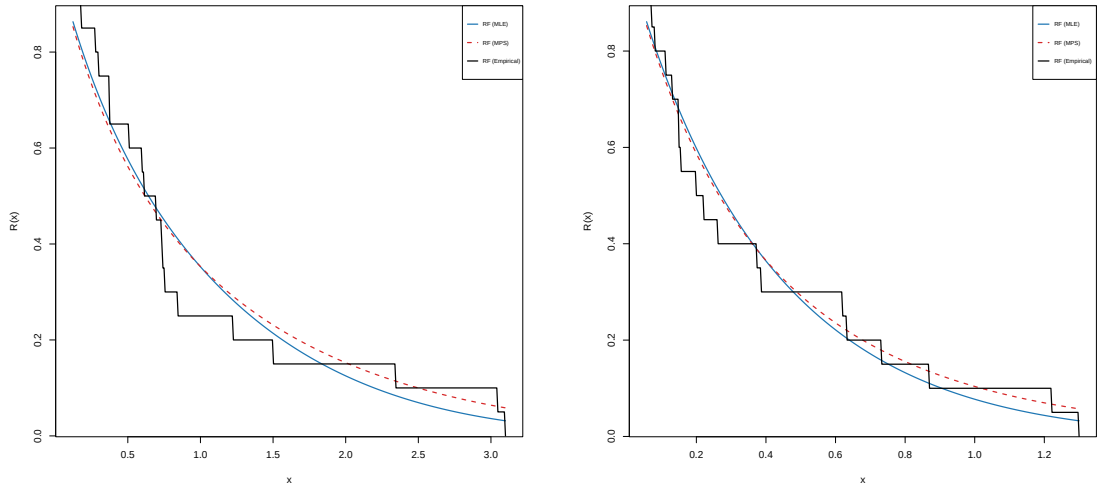

52.5kV 55kV

Figure 4: RF plots for the real dataset at stress levels 52.5kV and 55kV.

Before proceeding with further analysis, it is also important to verify whether the two stress levels in the dataset share a common shape parameter θ. This assumption is examined using a likelihood ratio test. The test statistic is defined as $\Lambda = 2\,(l_1 + l_2 - l_c)$, where l_1 and l_2 denote the maximized log-likelihood values at stress levels 1 and 2, respectively, and l_c is the maximized log-likelihood obtained under the constraint of a common shape parameter. Under the null hypothesis of equal shape parameters, Λ approximately follows a chi-square distribution with one degree of freedom, i.e., $\Lambda \dot{\sim} \chi^2_1$. For the dataset, the test value is $\Lambda = 2.250204$ with a corresponding p-value of 0.133597. Since $p > 0.05$, the null hypothesis of equal shape parameters is not rejected. Therefore, there is no statistically significant evidence that θ differs between the two stress levels, which supports the use of a common shape parameter

for the Hj model at the 5% significance level.

For illustrative purposes, a Type-II censored CSALT dataset is considered with $r_1 = 15$ and $r_2 = 15$. The parameters of the Hj distribution are then estimated at the different stress levels using the two methods described earlier. The resulting parameter estimates, together with their SEs, are reported in Table 10. From Table 10, it is observed that the estimated scale parameters λ_i $(i = 1, 2)$ increase as the stress level increases. In addition, the estimated RF, HRF, and the scale parameter at the normal stress level $s_u = 50$ are obtained for this dataset, and the corresponding results are summarized in Table 11. For both estimation methods, the estimated scale parameter at the use stress level is smaller than the estimates obtained at the higher stress levels. Table 12 presents the ACIs along with their corresponding interval widths. The ACIs based on the MLEs yield shorter interval widths for all parameters, except θ and the RF, compared with those obtained using the MPSEs. It should be emphasized that these findings are specific to the present dataset and may not necessarily extend to other datasets or alternative lifetime models. Figure 5 depicts the profile log-likelihood functions for a, b, and θ. For the current dataset, each profile curve exhibits a single, well-defined maximum near the corresponding estimate, indicating that the MLEs exist and are unique. The unimodal profiles also support parameter identifiability and the numerical stability of the proposed estimation procedures. Since the remaining profiles using the MPSEs display behavior similar to that shown in Figure 5, they are omitted to avoid repetition.

Table 10: Parameter estimates and SEs for the real dataset.

Parameter	MLE		MPS	
	Estimate	SE	Estimate	SE
a	-16.019325	16.230719	-11.999097	28.137967
b	0.317609	0.304134	0.231040	0.529606
θ	1.178797	0.585833	1.547607	0.578285
λ_1	1.925469	1.203007	1.139403	1.110670
λ_2	4.259677	3.251787	2.030140	2.768446

Table 11: The estimated reliability measures and scale parameter and their SEs under usual stress for the real dataset.

Parameter	t	MLE		MPSE	
		Estimate	SE	Estimate	SE
$R_u(t)$	0.4	0.627344	0.122331	0.564460	0.113497
	0.8	0.378555	0.156968	0.328146	0.152916
	1.2	0.210960	0.161925	0.186253	0.168477
$H_u(t)$	0.4	1.190140	0.510615	1.361227	0.575705
	0.8	1.351171	0.800205	1.371368	0.959508
	1.2	1.580243	1.182457	1.470837	1.421862
λ_u	-	0.870355	1.012823	0.639483	1.204340

Table 12: The interval bounds and the interval length for the real dataset.

Parameter	MLE		MPSE	
	Interval Bound	Interval Length	Interval Bound	Interval Length
a	(-47.83095 , 15.79230)	63.62325	(-67.14850 , 43.15030)	110.2988
b	(-0.278482 , 0.913701)	1.192183	(-0.806968 , 1.269048)	2.076016
θ	(0.030585 , 2.327009)	2.296424	(0.414189 , 2.681025)	2.266836
λ_u	(0.000000 , 2.855452)	2.855452	(0.000000 , 2.999945)	2.999945
$R_u(0.4)$	(0.387580 , 0.867107)	0.479527	(0.342009 , 0.786911)	0.444902
$R_u(0.8)$	(0.070903 , 0.686207)	0.615304	(0.028437 , 0.627855)	0.599418
$R_u(1.2)$	(0.000000 , 0.528328)	0.528328	(0.000000 , 0.516461)	0.516461
$H_u(0.4)$	(0.189352 , 2.190928)	2.001576	(0.232865 , 2.489588)	2.256723
$H_u(0.8)$	(0.000000 , 2.919544)	2.919544	(0.000000 , 3.251969)	3.251969
$H_u(1.2)$	(0.000000 , 3.897817)	3.897817	(0.000000 , 4.257636)	4.257636

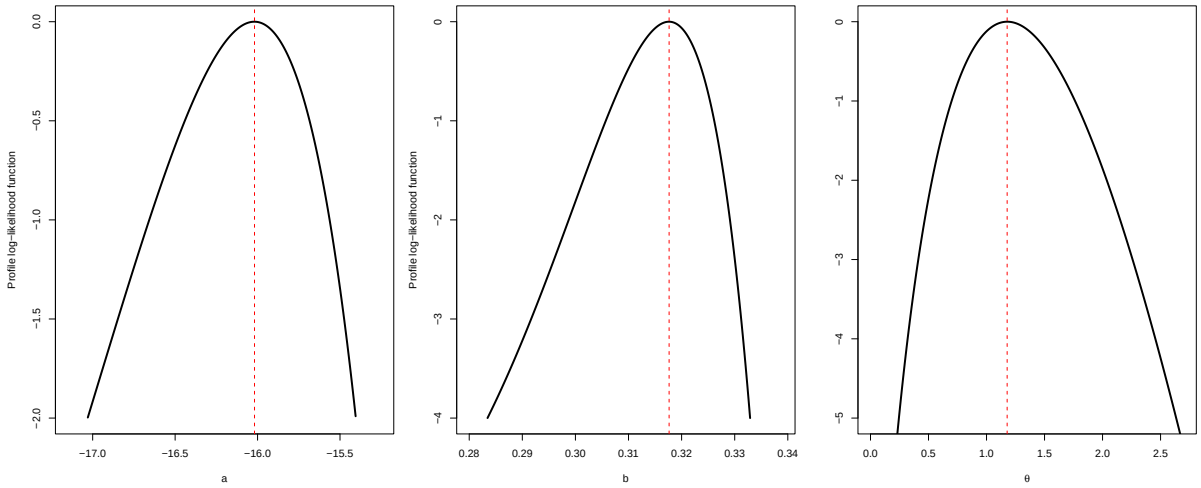

Figure 5: Profile log-likelihood functions for a, b, and θ using the dataset.

7 Conclusions

This study investigated reliability estimation for the Hjorth distribution under constant-stress accelerated life testing with Type-II censoring. Statistical inference is developed for the model parameters, the reliability function, and the hazard rate function using two classical approaches, namely the maximum likelihood estimation method and the maximum product of spacings estimation method. The methodology combined analytical derivations with numerical implementation, including a comprehensive simulation study and an application to a real engineering dataset. The simulation results provide several important insights. For parameter estimation, the maximum likelihood method generally yields more accurate estimates, as reflected by smaller bias and root mean square error values. In contrast, for reliability measures evaluated under normal operating conditions, the maximum product of spacings method demonstrates superior performance, particularly in estimating the scale parameter, the reliability function,

and the hazard rate function. The results also confirm that increasing the number of observed failures improves the overall accuracy and stability of both estimation procedures. Regarding interval estimation, the maximum product of spacings method typically produces shorter confidence intervals for reliability measures, while maintaining satisfactory coverage probabilities.

The real-data analysis further supports the applicability of the proposed model. The Hjorth distribution provides an adequate fit to the observed failure times, confirming its flexibility in capturing different lifetime behaviors. In addition, the estimated scale parameter increases with the stress level, which is consistent with the expected effect of accelerated conditions on lifetime characteristics. Overall, the findings indicate that the two estimation methods play complementary roles. The maximum likelihood method is more suitable for estimating model parameters, whereas the maximum product of spacings method offers advantages in estimating reliability measures under normal use conditions. The results also demonstrate that the Hjorth distribution, due to its flexibility in modeling various hazard rate shapes, provides an effective framework for analyzing accelerated life testing data with Type-II censoring in engineering and reliability applications.

Although the proposed methodology provides useful inferential results for the Hjorth distribution under Type-II censored constant-stress accelerated life test data, the study has some limitations. First, the analysis is based on a log-linear stress–life relationship, which assumes a specific form for the effect of stress on the scale parameter. Although this relationship is commonly used in accelerated life tests, other stress–life models may be more appropriate in certain practical applications. Second, the shape parameter is assumed to be common across all stress levels, implying that stress affects only the scale parameter while the general shape of the lifetime distribution remains unchanged. Third, the current study considers a single accelerating stress variable and focuses on a constant-stress accelerated life testing scheme.

Future research may extend the proposed framework in several directions. One possible extension is to investigate the Hjorth distribution under step-stress accelerated life testing, where the stress level changes during the experiment. Another important direction is to develop optimal constant-stress accelerated life testing designs for the Hjorth model, including the selection of stress levels, allocation of test units, and termination rules. Further work may also consider multiple-stress accelerated life testing models for applications involving more than one accelerating factor, such as temperature and voltage. In addition, alternative stress–life relationships may be explored to assess the robustness of the proposed inference procedures under different acceleration assumptions.

Acknowledgments

The authors would like to express their gratitude to the editor and anonymous referees for valuable suggestions and helpful observations.

Availability of Data and Materials:

The data that support the findings of this study are available within the paper.

Conflicts of Interest:

The authors declare no conflicts of interest to report regarding the present study.

Author Contributions

All authors contributed to this work equally. All authors reviewed the manuscript.

AI Usage Statement:

No AI-based tools were used in the generation, writing, revising, analysis, or interpretation of the research data and findings presented in this article.

References

[1] Meeker, W. Q., Escobar, L. A., & Pascual, F. G. (2021). *Statistical methods for reliability data*. New York: John Wiley & Sons.

[2] Nelson, W. B. (2009). *Accelerated testing: statistical models, test plans, and data analysis*. New York: John Wiley & Sons.

[3] Abd El-Raheem, A. M. (2019). Optimal plans and estimation of constant-stress accelerated life tests for the extension of the exponential distribution under type-I censoring. Journal of Testing and Evaluation, 47(5), 3781-3821. doi:10.1520/JTE20170553.

[4] Kumar, D., Nassar, M., Dey, S., & Alam, F. M. A. (2022). On estimation procedures of constant stress accelerated life test for generalized inverse Lindley distribution. Quality and Reliability Engineering International, 38(1), 211-228. doi:10.1002/qre.2971.

[5] Wu, W., Wang, B. X., Chen, J., Miao, J., & Guan, Q. (2023). Interval estimation of the two-parameter exponential constant stress accelerated life test model under Type-II censoring. Quality Technology & Quantitative Management, 20(6), 751-762. doi:10.1080/16843703.2022.2147688.

[6] Kamal, M., Khan, S., Rahman, A., Aldallal, R. A., El-Raouf, M. A., Muse, A. H., & Rabie, A. (2022). Reliability analysis of hybrid system using geometric process in multiple level of constant stress accelerated life test through simulation study for Type-II progressive censored masked data. Mathematical Problems in Engineering, 2022(1), 9528479. doi:10.1155/2022/9528479.

[7] Elwahab, M. E. A., Alqasem, O. A., & Nassar, M. (2025). Analysis and applications of Nakagami constant-stress model using progressive type-II censored data. Physica Scripta, 100(3), 035206. doi:10.1088/1402-4896/adae3d.

[8] Lou, Y., Zheng, H., & Yang, J. (2023). Optimal design of reliability acceptance sampling plan based on constant-stress accelerated life testing considering the uncertainty of accelerated factor. Quality and Reliability Engineering International, 39(4), 1318-1333. doi:10.1002/qre.3295.

[9] Babu, S. (2025). Generalized Marshall-Olkin bivariate exponential distribution and its application in constant-stress accelerated life test. International Journal of System Assurance Engineering and Management, 16(10), 3463-3480. doi:10.1007/s13198-025-02871-9.

[10] Balakrishnan, N., Castilla, E., & Ling, M. H. (2022). Optimal designs of constant-stress accelerated life-tests for one-shot devices with model misspecification analysis. Quality and Reliability Engineering International, 38(2), 989-1012. doi:10.1002/qre.3031.

[11] Liu, J., Wang, L., Tripathi, Y. M., & Lio, Y. (2024). Inference of constant-stress model of Fréchet distribution under a maximum ranked set sampling with unequal samples. Axioms, 13(6), 394. doi:10.3390/axioms13060394.

[12] Balakrishnan, N., Jaenada, M., & Pardo, L. (2026). Robust divergence-based tests of hypotheses for simple step-stress accelerated life-testing under Gamma lifetime distributions. Journal of Computational and Applied Mathematics, 117362. doi:10.1016/j.cam.2026.117362.

[13] LA, Q. T., Valis, D., Vintr, Z., Gajewski, J., Žák, L., Kohl, Z., & Cu, X. P. (2026). An approach to analyse of LED degradation heterogeneity in step-stress accelerated testing. Eksploatacja i Niezawodność–Maintenance and Reliability, 28(3):217551. doi:10.17531/ein/217551.

[14] Ling, M. H., Cramer, E., & Bae, S. J. (2025). Statistical inference and optimal design for step-stress accelerated life testing with hybrid group censoring for non-destructive one-shot devices. Reliability Engineering & System Safety, 111506. doi:10.1016/j.ress.2025.111506.

[15] Rather, R. A., & Ahmad, A. (2025). Bayesian reliability estimation for Copoun distribution using type II censored step-stress accelerated life tests: methods and applications. Sequential Analysis, 44(4), 427-450. doi:10.1080/07474946.2025.2531386.

[16] Das, R., Mani Tripathi, Y., Wang, L., & Wu, S. J. (2025). Inference for simple step stress accelerated life test model under progressively censored Gompertz data. Applied Stochastic Models in Business and Industry, 41(5), e70037. doi:10.1002/asmb.70037.

[17] Shiha, F. A., Aldawsari, A. M., Alotaibi, R., & Magar, A. M. (2026). Transmuted one-parameter Sarhan-Tadj-Hamilton distribution: properties and applications. Mathematical Sciences, 20(1), 1-18. doi:10.57647/mathsci.2025.1904.18008.

[18] Atchadé, M. N., Agbahide, A. A., Otodji, T., Bogninou, M. J., & Moussa Djibril, A. (2025). A new shifted Lomax-X family of distributions: properties and applications to actuarial and financial data. Computational Journal of Mathematical and Statistical Sciences, 4(1), 41-71. doi:10.21608/cjmss.2024.307114.1066.

[19] Sayibu, S. B., Luguterah, A., & Nasiru, S. (2024). Mcdonald generalized power weibull distribution: properties, and applications. J. Stat. Appl. Probab, 13, 297-322. doi:10.18576/jsap/130121.

[20] Gaire, A. K., & Gurung, Y. B. (2024). Skew log-logistic distribution: properties and application. Statistics in Transition new series, 25(1), 43-62. doi:10.59170/stattrans-2024-003.

[21] Hjorth, U. (1980). A reliability distribution with increasing, decreasing, constant and bathtub-shaped failure rates. Technometrics, 22(1), 99-107. doi:10.2307/1268388.

[22] Guess, F., & Nam, K. H. (1998). Failure rate and mean residual life with trend changes. Asia-Pacific Journal of Operational Research, 15(2).

[23] Yadav, A. S., Bakouch, H. S., & Chesneau, C. (2020). Bayesian estimation of the survival characteristics for Hjorth distribution under progressive type-II censoring. Communications in Statistics-Simulation and Computation, 51(3), 882-900. doi:10.1080/03610918.2019.1659363.

[24] Pandey, R., & Ali, D. (2021). Bayesian analysis of Hjorth distribution under generalised Type I progressive hybrid censoring scheme. Journal of Scientific Research, 65, 191-201. doi:10.37398/JSR.2021.650323.

[25] Elshahhat, A., and Nassar, M. (2021). Bayesian survival analysis for adaptive Type-II progressive hybrid censored Hjorth data. Computational Statistics, 36(3), 1965-1990. doi:10.1007/s00180-021-01065-8.

[26] Alotaibi, R., Nassar, M., & Elshahhat, A. (2025). Statistical computation of Hjorth competing risks using binomial removals in adaptive progressive Type II censoring. Mathematics, 13(12), 2010. doi:10.3390/math13122010.

[27] Ver Hoef, J. M. (2012). Who invented the delta method?. The American Statistician, 66(2), 124-127. doi:10.1080/00031305.2012.687494.

[28] Bera, A. K., & Koley, M. (2023). A history of the delta method and some new results. Sankhya B, 85(2), 272-306. doi:10.1007/s13571-023-00305-9.

[29] Cheng, R. C. H., & Amin, N. A. K. (1983). Estimating parameters in continuous univariate distributions with a shifted origin. Journal of the Royal Statistical Society: Series B (Methodological), 45(3), 394-403. doi:10.1111/j.2517-6161.1983.tb01268.x.

[30] Ghosh, K., & Jammalamadaka, S. R. (2001). A general estimation method using spacings. Journal of Statistical Planning and Inference, 93(1-2), 71-82. doi:10.1016/S0378-3758(00)00160-9.

[31] Anatolyev, S., & Kosenok, G. (2005). An alternative to maximum likelihood based on spacings. Econometric Theory, 21(2), 472-476. http://www.jstor.org/stable/3533475.

[32] Singh, R. K., Kaushik, A., Singh, S. K., & Singh, U. (2018). Product spacings for the estimation of the parameters of the exponentiated Pareto distribution. International Journal of Applied Mathematics & Statistics, 57, 79-95. http://www.ceser.in/ceserp/index.php/ijamas/article/view/5478.

[33] Almetwally, E. M., Almongy, H. M., Rastogi, M. K., & Ibrahim, M. (2020). Maximum product spacing estimation of Weibull distribution under adaptive type-II progressive censoring schemes. Annals of Data Science, 7(2), 257-279. doi:10.1007/s40745-020-00261-5.

[34] Du, S., & Gui, W. (2025). Model comparison and parameter estimation for Gompertz distributions under constant stress accelerated lifetime tests. Applied Sciences, 15(16), 9199. doi:10.3390/app15169199.

[35] University of Waterloo (Ontario). Department of Electrical Engineering, & Stone, G. C. (1978). Statistical analysis of accelerated aging tests on solid electrical insulation. University of Waterloo: Waterloo, ON, Canada.

Disclaimer / Publisher's Note:
The statements and data in all publications are solely those of the author(s) and contributor(s) and do not necessarily reflect the views of the publisher. The publisher accepts no responsibility for any injury to people or property resulting from any ideas, methods, instructions or products referred to in the content.